IOPscience iopscience.iop.org

Home Search Collections Journals About Contact us My IOPscience

Vacancies in wurtzite GaN and AlN

This article has been downloaded from IOPscience. Please scroll down to see the full text article.

2009 J. Phys.: Condens. Matter 21 015803

(http://iopscience.iop.org/0953-8984/21/1/015803)

View the table of contents for this issue, or go to the journal homepage for more

Download details:
IP Address: 129.252.86.83
The article was downloaded on 29/05/2010 at 16:55

Please note that terms and conditions apply.

IOP PUBLISHING JOURNAL OF PHYSICS: CONDENSED MATTER

J. Phys.: Condens. Matter **21** (2009) 015803 (6pp) doi:10.1088/0953-8984/21/1/015803

Vacancies in wurtzite GaN and AlN

K Laaksonen, M G Ganchenkova and R M Nieminen

Laboratory of Physics, Helsinki University of Technology, PO Box 1100, FI-02015 HUT, Finland

E-mail: kml@fyslab.hut.fi

Received 21 October 2008, in final form 13 November 2008
Published 8 December 2008
Online at stacks.iop.org/JPhysCM/21/015803

Abstract

Vacancies in wurtzite GaN and AlN are studied using a computational method which is based on the density functional theory (DFT) and takes into account the errors arising from use of finite-sized supercells and the DFT band gap underestimation. Negatively charged N vacancies in GaN and AlN are found to be stable, with formation energies similar to and higher than those of Ga and Al vacancies in n-type material under Ga- and Al-rich growth conditions, respectively. The localization and energies of the defect levels close to the computational conduction band edge are considered in detail.

1. Introduction

GaN and AlN are important wide-band-gap semiconductors for micro- and optoelectronic applications, such as light emitting devices operating in the blue or ultraviolet spectral regions. Defects can significantly affect the material properties and the research on the native defects in these materials has a long history (see recent reviews for an up-to-date summary [1, 2]). Among the most intensively studied defects are atomic vacancies due to their important effects on the material properties. In particular, the positively charged nitrogen vacancy was initially considered a strong candidate for being responsible for the n-type conductivity in as-grown GaN [3, 4]. However, later calculations revealed that the formation energy of the nitrogen vacancy V_N in n-type material is too high for it to exist in the required abundance in thermal equilibrium [5–7]. Currently, it is assumed that the GaN crystals become contaminated during the growth process by oxygen, which provides the charge carriers.

Since the work by Neugebauer and Van de Walle [5], Ga vacancies (V_{Ga}) have been considered to be the only native defects to exist in observable amounts in as-grown GaN. The nitrogen vacancies were expected to play a role in the defect microstructure kinetics only in p-doped material [1]. However, it has been proposed recently that nitrogen vacancies, including negatively charged ones, and their complexes (e.g. mixed Ga–N divacancies), can also be important participants in the defect kinetics in n-type GaN [8]. Most of the computational studies, to our knowledge, have been performed for the zinc-blende structure, even though the main polytype of GaN is wurtzite.

For AlN the situation is similar. Indeed, several theoretical studies concerning vacancies and impurities in the zinc-blende polytype of AlN (see, for example, [7, 9, 10] and the references therein) have been published over the years, but only very recently have there been studies which have concentrated on the wurtzite AlN [11–14]. In [10] it was shown that the defect levels induced by the N vacancy in the upper part of the band gap exhibit different behaviour in the zinc-blende and wurtzite structures. They are in resonance with the conduction band in the zinc-blende structure while in wurtzite they lie well below the conduction band edge. The negative charge states, however, were not discussed in more detail. A recent study [12], which concentrated mainly on p-type doping, investigated the properties of native defects and impurities in wurtzite AlN with only positive and neutral charge states reported for the N vacancy. In [11] and [13] the nitrogen vacancy was also studied in the negative charge states in wurtzite AlN, but in the former they were found to be unimportant because of the high formation energy.

Most of the previous calculations have been performed for supercells of size less than 96 atoms, which may be too small to reach converged results, especially in the case of GaN, which has d electrons with long-range nature. In this paper we consider the convergence of the formation energy with the supercell (SC) size (with calculations done for SCs with up to 300 atoms) for neutral and charged vacancies in *wurtzite* GaN and AlN. The transition levels of the different types of vacancies are estimated based on the formation energies obtained for the infinite crystal.

2. Computational details

Total-energy calculations have been performed using the density functional based VASP code. Since Ga is a transition

 © 2009 IOP Publishing Ltd Printed in the UK

metal with relatively weakly bound d electrons, they need to be adequately represented and were treated explicitly using the projector augmented wave (PAW) method [15]. The same method was also used for AlN. For the exchange–correlation energy the local spin density (LSDA) approximation [16] was used, since we found that it gives a better description of GaN and AlN properties than other popular approximations (e.g. generalized gradient functionals).

In this work the wurtzite structure, which is the main polytype of both GaN and AlN, is used in all calculations. The lattice parameters a and c were selected based on minimization of the energy of the perfect lattice, and the minimum energy was achieved at $a = 3.15$ Å and $c/a = 1.632$ for GaN (experiments: $a = 3.19$ Å and $c/a = 1.626$ [17]) and $a = 3.09$ Å and $c/a = 1.601$ for AlN (experiments: $a = 3.11$ Å and $c/a = 1.601$ [18]). These values were used in all subsequent calculations with bulk and defect-containing supercells.

Defects were created by the removal of a lattice atom of an appropriate type. During structural optimization the atoms were allowed to relax until the residual forces fell below 0.01 eV Å^{-1}. In the charged defect cases a uniform, neutralizing 'jellium' background charge was used.

The formation energies of the defects were determined according to the Zhang–Northrup formalism [19]. In this approach, the formation energy of a vacancy with the charge q is

$$E_{\mathrm{f}}^{\mathrm{def}} = E_{\mathrm{tot}}^{\mathrm{def}} - E_{\mathrm{tot}}^{\mathrm{bulk}} + \mu_i + q[E_{\mathrm{V}}^{\mathrm{def}} + \mu_{\mathrm{e}}] \qquad (1)$$

where $E_{\mathrm{tot}}^{\mathrm{def}}$ is the total energy of the supercell containing a vacancy, $E_{\mathrm{tot}}^{\mathrm{bulk}}$ is the total energy of the ideal supercell, μ_i is the chemical potential corresponding to the removed atom, $E_{\mathrm{V}}^{\mathrm{def}}$ is the valence band maximum for the defect supercell and μ_{e} is the electron chemical potential (with zero at the valence band maximum). If the formation energy is calculated in the infinite crystal, $E_{\mathrm{V}}^{\mathrm{def}}$ is equal to the valence band maximum in the bulk $E_{\mathrm{V}}^{\mathrm{bulk}}$, which can be then used instead without any additional corrections. The chemical potentials of the removed atoms were calculated using the chemical potentials of the N_2 molecule and bulk Al, Ga, AlN and GaN depending on the assumed growth conditions (Al, Ga or N rich) [1].

The formation energy is greatly affected by the fact that all calculations are performed using periodically repeated finite-sized supercells which contain up to a few hundred atoms. This periodic replication can introduce artificial long-range elastic and electrostatic interactions between the periodic defect images. However, if the supercell size could be increased enough, the interaction of the defect with the spurious periodic images and with the jellium background would become negligible.

The finite-size effects were taken into account in the formation energy calculations by considering the change in configuration energy $E_{\mathrm{c}}^{\mathrm{def}} = E_{\mathrm{tot}}^{\mathrm{def}} - E_{\mathrm{tot}}^{\mathrm{bulk}}$ with the increase of the supercell size. Both GaN and AlN were considered in the wurtzite structure, which is non-cubic, and the distance between the defect and its image is different in different directions (a and c). The use of the wurtzite structure makes it difficult to generate a sufficiently large set of supercells with computationally feasible size and exactly the same symmetry. Thus we have calculated the configuration energy in a number of different supercell sizes with different symmetries. Supercells of 32, 72, 96, 108, 128, 192 and 300 atoms were used for GaN and 96 and 300 atom for AlN. Brillouin-zone sampling was done in the range of $6 \times 6 \times 6$ to $2 \times 2 \times 2$ Monkhorst–Pack **k**-point sets depending on the considered SC. The cation and anion vacancies were considered in charge states from $+3$ to -3 for both GaN and AlN.

Both GaN and AlN are wide-band-gap materials with the experimental band gaps of $E_{\mathrm{g}}^{\mathrm{GaN}} = 3.47$ eV [20] and $E_{\mathrm{g}}^{\mathrm{AlN}} = 6.12$ eV [21], respectively. However, in the calculations the band gaps are underestimated and in our case the Kohn–Sham band gaps are $E_{\mathrm{g}}^{\mathrm{GaN}} = 2.2$ eV and $E_{\mathrm{g}}^{\mathrm{AlN}} = 4.4$ eV. Therefore, the total energies used in the calculation of the configuration energies were corrected for the LDA band gap error by using the so-called 'scissor' operator. It works by 'stretching' the underestimated theoretical band gap to the size of the experimental one. The scissor-operator correction arising from occupied defect levels to the total energy of the defect supercell was calculated from the difference of the band gap in experiments ($E_{\mathrm{g}}^{\mathrm{exp}}$) and in the defect supercell ($E_{\mathrm{g}}^{\mathrm{def}}$):

$$E_{\mathrm{scissor}} = \frac{E_{\mathrm{level}} - E_{\mathrm{V}}^{\mathrm{bulk}}}{E_{\mathrm{g}}^{\mathrm{def}}} (E_{\mathrm{g}}^{\mathrm{exp}} - E_{\mathrm{g}}^{\mathrm{def}}) \qquad (2)$$

where E_{level} is the Kohn–Sham (KS) energy of the defect level and $E_{\mathrm{V}}^{\mathrm{bulk}}$ the valence band maximum (VBM) in the bulk supercell at the Γ-point. The correction shifts the defect levels proportionally to their distance from the valence band maximum. It has been applied for every occupied defect level located near the conduction band minimum (CBM) but not for those derived from valence band states. It is thus applied for the N vacancies in neutral and negative charge states but not for Ga, Al and positive N vacancies, which do not have occupied levels near the CBM.

3. Results and discussion

The configuration energies (including the scissor corrections) for the neutral and negative N and Ga vacancies in GaN are shown as a function of the inverse supercell volume (V) in figure 1 for the 96, 108, 128, 192 and 300 atom supercells (32 and 72 atom SCs give strongly nonlinear behaviour so they were not considered). The figure also shows the estimated dependences which have been used in the extrapolation to the infinite crystal. A similar procedure was used also for the other charge states and defects in AlN. The found configuration energies corresponding to the infinite crystal were used to calculate the formation energies which are given in table 1 for cation-rich growth conditions.

Taking into account the finite-size effects can be important in order to obtain the qualitatively correct results. In particular, the increase of the supercell size can lead to a change in the ordering of the energies of the different types of vacancies: for the small SCs the V_{Ga}^{-3} formation energy is essentially smaller than that for the V_{N}^{-3}, whereas for the large SCs V_{N}^{-3} becomes more energetically favourable with similar formation

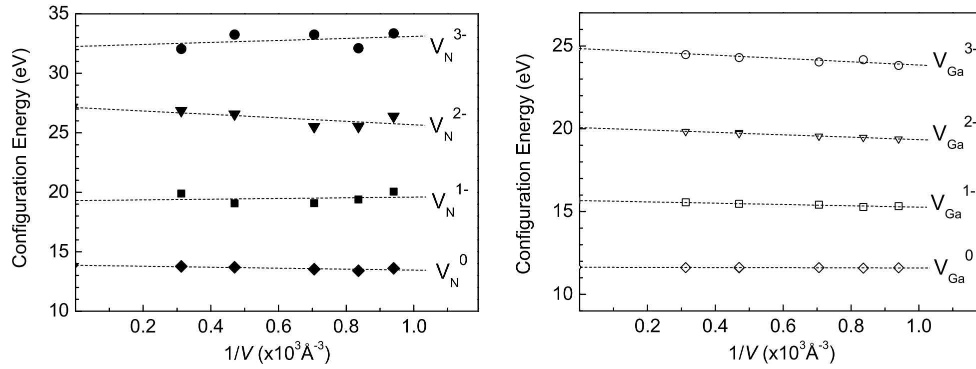

Figure 1. Configuration energies of N (left) and Ga (right) vacancies in GaN in neutral and negative charge states. Lines are guides to the eye for the estimation of the configuration energy in the infinite crystal.

Table 1. The formation energies (in eV) in an infinite crystal for the most important charge states of the different types of vacancies in GaN and AlN. The formation energies have been calculated from equation (1) assuming cation-rich growth conditions and the value of zero for the electron chemical potential.

	GaN		AlN	
Charge	V_N	V_{Ga}	V_N	V_{Al}
3	0.89		−1.86	10.41
2	0.95		−0.98	10.33
1	0.82		−0.45	10.22
0	3.16	8.40	4.60	10.20
−1	5.00	8.83	10.19	11.02
−2	8.45	9.60	15.71	12.16
−3	10.59	10.67	21.71	13.53

energy to V_{Ga}^{-3}. We also found out that for vacancies in GaN even a 300 atom SC is not enough for the full convergence of the defect energy.

The formation energies for the Ga and N vacancies in GaN and Al and N vacancies in AlN are shown as a function of the Fermi level position in figure 2. Both cation vacancies were found to have three transition levels in the band gap at 0.43 eV (neutral to −1 transition (0/−)), 0.77 eV (−/−2) and 1.07 eV (−2/−3) above the valence band maximum (VBM) for V_{Ga} and 0.82 eV (0/−), 1.14 eV (−/−2) and 1.37 eV (−2/−3) for V_{Al}. Under both Ga(Al)- and N-rich conditions the formation energy of the Ga(Al) vacancy is high for p-type material and low enough in n type to expect its formation in measurable concentration. Our results for AlN agree qualitatively well with [12] and for GaN with [1]. The most probable reasons behind the quantitative differences are the differences in the methodology used in the calculations such as the use of the finite-size corrections in our case.

An essentially different situation is encountered in the case of the nitrogen vacancy, which was also considered in charge states ranging from +3 to −3. The most important conclusion that follows from our results for GaN is that the nitrogen vacancy is a negative-U defect that exists, depending on the Fermi level position, either in the singly positive or in singly to triply negative charge states. Another important conclusion is that under Ga-rich conditions (which are the typical growth conditions) V_N is energetically more favourable than V_{Ga} over the whole band gap and not only in p-type material, as has been assumed earlier [1]. One more difference between the present results and the ones published earlier [1] is that according to our calculations only a singly positive charge state for V_N exists in p-type material. In contrast to this, the previous calculations also showed the stability of the triply positively charged vacancy in the deep p-type region. Our analysis showed, however, that this can be the case if the defect energy convergence is not reached, since according to our calculations V_N^{+3} becomes unstable in the infinite GaN crystal.

The values for the transition level positions for N vacancies in GaN are (+/−) at 2.09 eV and (−/−3) at 2.80 eV and in AlN (+3/+) at 0.71 eV, (+/0) at 5.05 eV, (0/−2) at 5.56 eV and (−2/−3) at 6.00 eV when the VBM is taken as the reference. Similar to GaN, in AlN V_N also exhibits negative-U behaviour but with only one transition of this type, namely (+3/+). For the (0/−2) transition the formation energies of the N vacancies in charge states −1, −2 and −3 for Fermi level values near the (0/−2) transition are very close to each other (within a few 0.1 eV), which makes it difficult to confirm, for example, the instability of the −1 charge state for V_N.

In contrast to GaN, in AlN under Al-rich conditions the N vacancy has a low formation energy in p-type material but a rather high one in n type. For the N-rich conditions V_N has lower formation energy in p-type material than V_{Al}, which is, however, clearly more favourable in the case of n-type material. These observations together with the (+3/+) transition and the +1 charge state for V_N in a wide range of Fermi energies agree well with the previous results [10–12], with the exception that in [13] V_N was found to be important in n-type material under Al-rich conditions. In agreement with [11, 13] we find stable negative charge states for the N vacancy in AlN high in the band gap, which have not been considered in, for example, [12]. Also, the positions of the transition levels involving neutral and negative V_N are closer to the CBM than in [11, 13]. These differences can be explained by the inclusion of the finite-size and scissor corrections in our calculations, since, for example, the scissor operator increases the formation energies and lifts the transition levels higher in the band gap for the neutral and negative N vacancies.

Some of the transition levels (calculated as total-energy differences) lie above the DFT single-particle gap for the bulk,

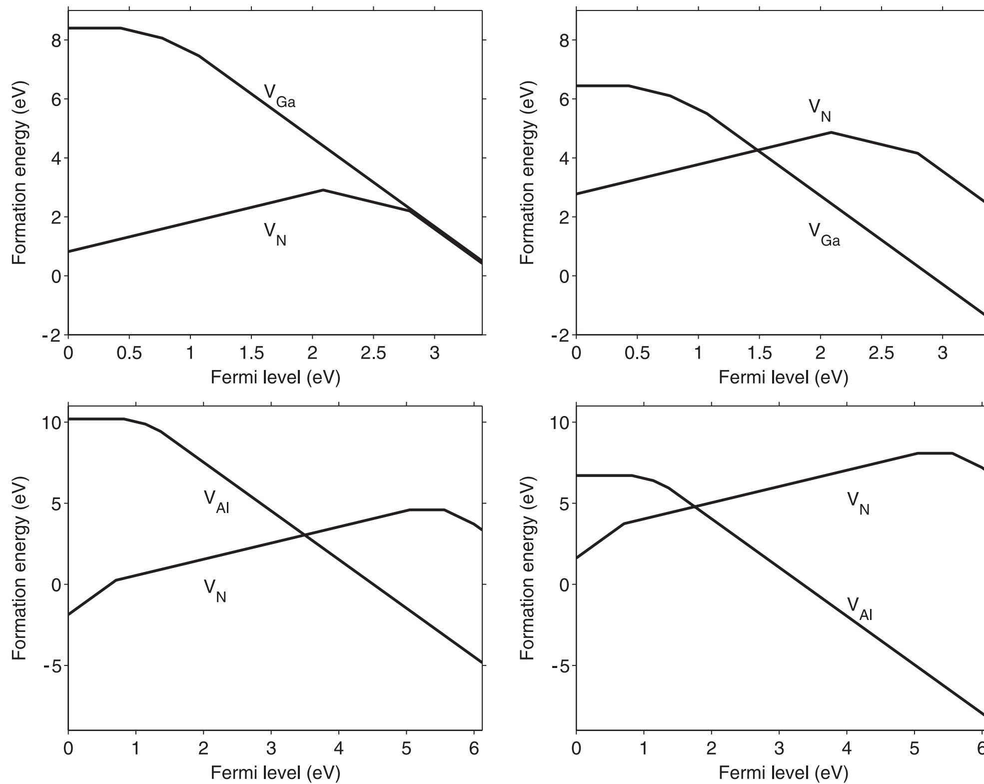

Figure 2. Formation energies of vacancies in different charge states versus Fermi level for Ga- (top left) and N-rich (top right) conditions in GaN, and Al- (bottom left) and N-rich (bottom right) conditions in AlN.

which means that they could be resonant with the conduction band in our calculations (see figure 2). However, the band structures of GaN and AlN with an N vacancy in figure 3 show that the defect levels for GaN and AlN are clearly localized in the band gap. The defect levels high in the band gap are relatively flat and close to, but still clearly separated from, the conduction band states in AlN. In GaN the two lowest defect levels are separated from the third one, which is very close to the conduction band.

In order to remove the uncertainties concerning the negative N vacancy states in GaN, the following analysis was performed. First, it is found that the filling of the defect levels is accompanied by changes in the relaxation and bonding patterns. When the charge state changes from V_N^+ to V_N^{-3}, the relaxation changes from outward (for V_N^+) to inward (for neutral and negative charge states). With each electron the inward relaxation increases, while the distance between the nearest neighbours and the vacancy falls: from 1.86/1.99 Å (first/second nearest neighbour in bulk) for V_N^+ to 1.68/1.77 Å for V_N^{-3}, while the equilibrium distance is ∼1.93 Å, in the case of GaN, and from 1.92/1.98 Å for V_N^+ to 1.66/1.77 Å for V_N^{-3}, while the equilibrium distance is 1.88/1.89 Å, in the case of AlN. Also, the symmetry decreases from V_N^+ to the negative charge states as the result of a Jahn–Teller distortion, which shows a bonding trend between the nearest neighbours of the vacancy. In turn, the bonding can be only due to the localization of the added electrons.

Indeed, the electron density distribution pattern of the highest occupied electron states clearly shows the localization of electrons in the defect as shown in figure 4 for GaN. As we can see from the figure, the charge distributions around V_N, V_{Ga} and the oxygen atom on substitutional N-site (O_N in the positive charge state, not considered in more detail in this paper) are qualitatively different. For both V_N and V_{Ga} the main part of the charge of the electrons on the highest occupied states is localized in the vicinity of the defects, even though the character of the distribution is different. In contrast, O_N, which is known to be a shallow donor with electron level resonant with the conduction band, manifests a much more widely spread distribution of the electron on the highest occupied state.

From the radial distribution we can also observe the very pronounced localization of the electrons occupying the highest KS levels within the sphere of the radius of approximately third nearest neighbour distance. Indeed, according to figures 4 and 5, in the case of V_N in GaN, 0.6–0.7 of an electron charge for charge states from 0 to −3 is localized within a sphere of radius 4 Å. For comparison, in the same figures the model conduction band electron distribution in the SC is shown as a thin dashed curve. In this case only 0.1 e is localized within the sphere of the same radius as above. A state corresponding to the valence band shows the same behaviour, which indicates that this model representation of the conduction electron is correct (positively charged V_N in GaN in figure 5).

The radial distribution of the electron on the highest occupied state for V_{Ga}^{-3} has the same character, with a localization of about 0.8 e within a 4 Å sphere. This correlates with the fact that V_{Ga} levels are much deeper than V_N ones. For O_N the localization of the electron on the highest occupied state in the neutral charge state is less than 0.3 e, which correlates

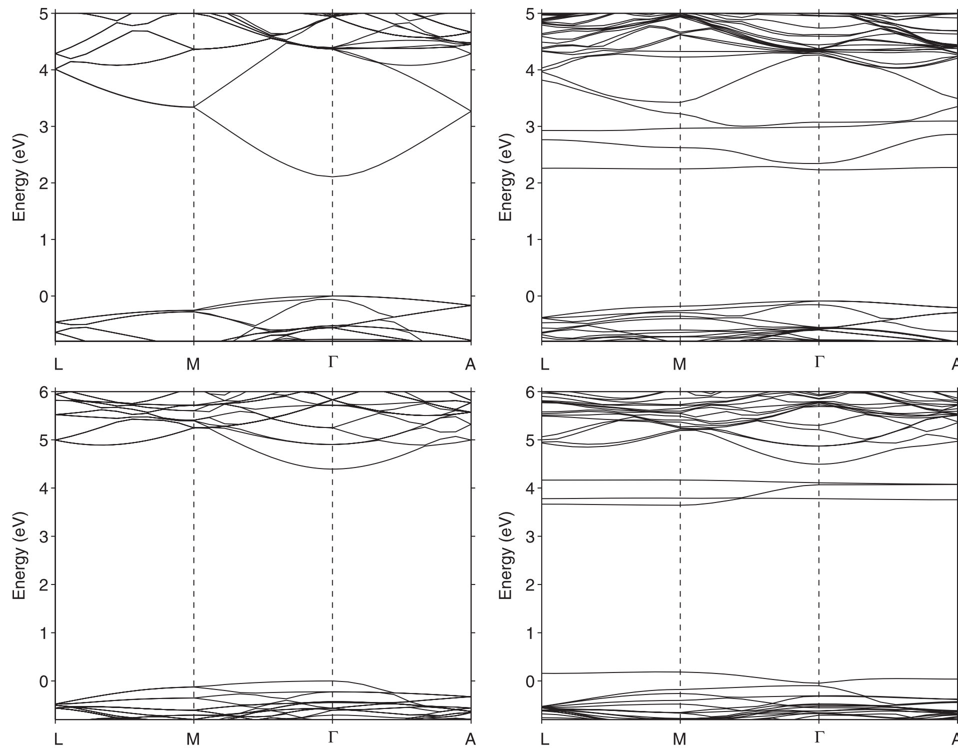

Figure 3. Band structure of the bulk (left column) and for one nitrogen vacancy in the SC (right column) for GaN (top row) and AlN (bottom row). The non-spin-polarized band structure is shown for clarity, although all other calculations were performed with spin polarization.

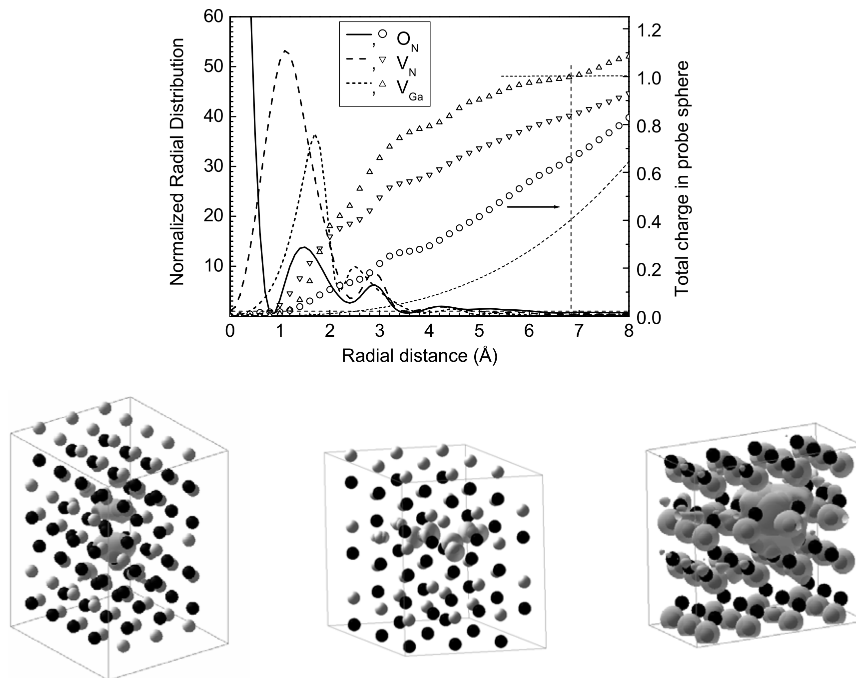

Figure 4. The electron radial distributions (top) and charge densities for N vacancy, Ga vacancy and O on substitutional N site in GaN (left to right on the bottom row, N shown as white and Ga as black spheres). The radial distance is given with respect to the centre of the vacancy with the dashed vertical line marking the minimum half-way distance between defect images. The thin dashed curve corresponds to a model conduction band electron.

with the fact that this level is resonant with the conduction band.

A comparison of the electron radial distributions for V_N in GaN and AlN shows that the localization is stronger in AlN (about 0.8 e) than in GaN (0.6–0.7 e). This correlates with the band structure, which in the case of AlN demonstrates a clear separation of the defect states from the conduction band. However, it should be noted that there is

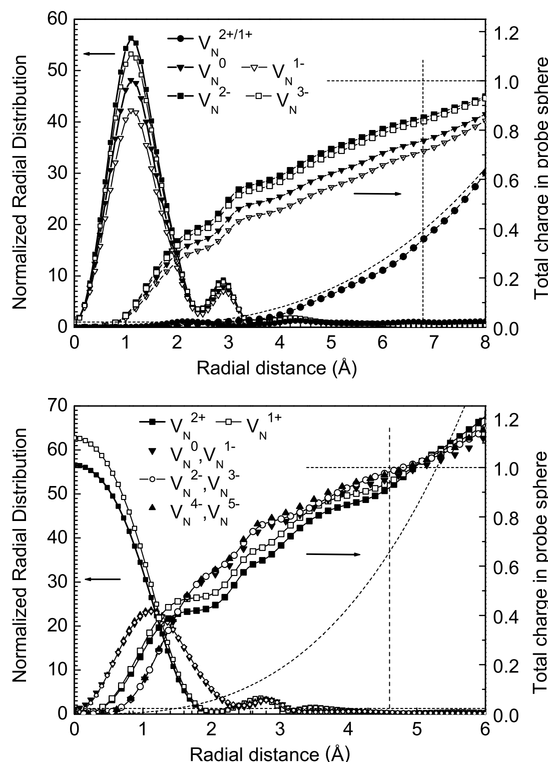

Figure 5. Electron radial distribution for nitrogen vacancy in GaN (top) and AlN (bottom). The radial distance is given with respect to the centre of the vacancy, with the dashed vertical line showing the minimum half-way distance between defect images. The thin dashed curve corresponds to a model conduction band electron.

an important difference between these two systems, namely that Ga is a d element, while Al is a p element. The d electrons have a long-range nature and are much more sensitive to the accuracy of the system description, such as the ion potential and the SC size, than the p electrons. This may be the source of the difference between the electron localization in GaN and AlN. The localization of the electron on the highest occupied level in V_N^0 was also studied in [13] for AlN, where it was found to be localized near the vacancy.

Despite the weaker localization of the N vacancy states in GaN, even the localization of about 0.6–0.7 e means that there is a potential well at the vacancy site and an activation energy is required to transfer the electron from the defect to the conduction band (see the comparison with the oxygen on the N site, where the state is resonant with the conduction band bottom). The existence of the activation energy implies a localization of the defect state within the band gap and the value of the localization allows us to suggest that the corresponding levels lie in the upper part of the gap close to the conduction band.

4. Conclusions

We have studied vacancies in GaN and AlN in the wurtzite structure using a density-functional-theory based method with finite-size and scissor corrections. N vacancies in GaN are found to be important defects at all Fermi energy values, and in the −3 charge state they have similar formation energies to Ga vacancies in n-type GaN. In AlN the N vacancy has stable negative charge states, with the corresponding transition levels located near the conduction band minimum. However, its formation energy in n-type material is high.

Acknowledgments

This research has been supported by the Academy of Finland through the Centres of Excellence Programme. We would like to thank the Center for Scientific Computing (CSC) in Finland for the computing facilities.

References

[1] Van de Walle C G and Neugebauer J 2004 *J. Appl. Phys.* **95** 3851
[2] Seebauer E G and Kratzer M C 2006 *Mater. Sci. Eng.* R **55** 57
[3] Maruska H P and Tietjen J J 1969 *Appl. Phys. Lett.* **15** 327
[4] Perlin P, Suski T, Teisseyre H, Leszczynski M, Grzegory I, Jun J, Porowski S, Bogusławski P, Bernholc J, Chervin J C, Polian A and Moustakas T D 1995 *Phys. Rev. Lett.* **75** 296
[5] Neugebauer J and Van de Walle C G 1994 *Phys. Rev.* B **50** 8067
[6] Mattila T, Seitsonen A P and Nieminen R M 1996 *Phys. Rev.* B **54** 1474
[7] Mattila T and Nieminen R M 1997 *Phys. Rev.* B **55** 9571
[8] Ganchenkova M G and Nieminen R M 2006 *Phys. Rev. Lett.* **96** 196402
[9] Vail J M, Chevrier D K, Pandey R and Blanco M A 2006 *J. Phys.: Condens. Matter* **18** 2125
[10] Stampfl C and Van de Walle C G 2002 *Phys. Rev.* B **65** 155212
[11] Ye H-G, Chen G-D, Zhu Y-Z and Lü H-M 2007 *Chin. Phys.* **16** 3803
[12] Zhang Y, Liu W and Niu H 2008 *Phys. Rev.* B **77** 035201
[13] Fara A, Bernardini F and Fiorentini V 1999 *J. Appl. Phys.* **85** 2001
[14] Hung A, Russo S P, McCulloch D G and Prawer S 2004 *J. Chem. Phys.* **120** 4890
[15] Kresse G and Joubert D 1999 *Phys. Rev.* B **59** 1758
[16] Perdew J P and Zunger A 1981 *Phys. Rev.* B **23** 5048
[17] Edgar J H, Strite S, Akasaki I, Amano H and Wetzel C (ed) 1999 *Gallium Nitride and Related Semiconductors* (London: INSPEC)
[18] Stampfl C and Van de Walle C G 1999 *Phys. Rev.* B **59** 5521
[19] Zhang S B and Northrup J E 1991 *Phys. Rev. Lett.* **67** 2339
[20] Bougrov V, Levinshtein M E, Rumyantsev S L and Zubrilov A 2001 *Properties of Advanced Semiconductor Materials GaN, AlN, InN, BN, SiC, SiGe* (New York: Wiley)
[21] Li J, Nam K B, Nakarmi M L, Lin J Y, Jiang H X, Carrier P and Wei S-H 2003 *Appl. Phys. Lett.* **83** 5163